Copy 7

RM A50J09a

RESEARCH MEMORANDUM

PRELIMINARY FLIGHT INVESTIGATION OF THE DYNAMIC LONGITUDINAL-STABILITY CHARACTERISTICS OF A 35° SWEPT-WING AIRPLANE

By William C. Triplett and
Rudolph D. Van Dyke, Jr.

Ames Aeronautical Laboratory
Moffett Field, Calif.

NATIONAL ADVISORY COMMITTEE
FOR AERONAUTICS

WASHINGTON
December 11, 1950

NATIONAL ADVISORY COMMITTEE FOR AERONAUTICS

RESEARCH MEMORANDUM

PRELIMINARY FLIGHT INVESTIGATION OF THE DYNAMIC LONGITUDINAL-STABILITY CHARACTERISTICS OF A 35° SWEPT-WING AIRPLANE

By William C. Triplett and
Rudolph D. Van Dyke, Jr.

SUMMARY

Flight measurements of the dynamic longitudinal-stability characteristics of a 35° swept-wing airplane are presented in this report. Pitching velocity responses to pulse-type elevator motions were recorded over a Mach number range of 0.60 to 1.04 at an altitude of approximately 35,000 feet. The measured period and damping of these oscillatory responses were used to compute the static stability parameter C_{m_α}, the factor $C_{m_q} + C_{m_{\dot{\alpha}}}$, and the number of cycles for the oscillations to damp to 1/10 amplitude. These results are compared with the same characteristics estimated from static wind-tunnel data.

The test results show a sharp reduction in damping at a Mach number of 0.92 with maximum damping occurring at Mach numbers of 0.88 and 0.94. Above 0.94 there is again a decrease in damping that continues over the remainder of the test range. The static stability increases rapidly with Mach number through the transonic range, except for a slight decrease at M = 0.92.

INTRODUCTION

At the present time there are only limited data available on the dynamic behavior of swept-wing aircraft, especially at transonic speeds. The flight-test program being conducted by the NACA on a 35° swept-wing airplane includes the determination of dynamic directional-, lateral-, and longitudinal-stability characteristics as affected by Mach number.

This report presents the preliminary results of a flight investigation into the longitudinal-stability characteristics of the test airplane. The simple method of analysis used here is possible because the airplane exhibits a lightly damped short-period oscillatory response. The computed flight-test characteristics are compared with estimations made from static wind-tunnel data.

More complete analyses, using additional flight data, are being carried out in order to determine the frequency responses of the airplane and the individual stability derivatives through the subsonic and transonic speed ranges.

SYMBOLS

C_L lift coefficient

C_m pitching-moment coefficient about airplane center of gravity

$C_{1/10}$ number of cycles required for oscillation to damp to 1/10 amplitude

I_y moment of inertia about Y axis, slug feet squared

M Mach number

P period of oscillation, seconds

S wing area, square feet

S_t horizontal-tail area, square feet

V velocity, feet per second

b damping coefficient

b_w wing span, feet

$\bar{c}$ wing mean aerodynamic chord $\left(\frac{\int_0^{b_w/2} c^2 dy}{\int_0^{b_w/2} c\, dy}\right)$, feet

c local wing chord, feet

i_t angle of incidence of horizontal tail, radians

[redacted]

k aerodynamic restoring moment

l_t tail length, feet

m mass, slugs

q pitching velocity, radians per second

t time, seconds

y distance from plane of symmetry, normal to plane of symmetry, feet

α angle of attack, radians

δ elevator deflection, radians

ϵ downwash angle, radians

η tail efficiency

ρ atmospheric density, slugs per cubic foot

$\frac{\rho V^2}{2}$ dynamic pressure, pounds per square foot

$\dot{\alpha}$ $\frac{d\alpha}{dt}$

$\dot{q}$ $\frac{dq}{dt}$

C_{L_α} $\frac{dC_L}{d\alpha}$

C_{m_α} $\frac{dC_m}{d\alpha}$

C_{m_q} $\frac{dC_m}{d(q\bar{c}/2V)}$

$C_{m_{\dot{\alpha}}}$ $\frac{dC_m}{d(\dot{\alpha}\bar{c}/2V)}$

M_α $C_{m_\alpha} S\bar{c} \frac{\rho}{2} V^2$

M_δ $\frac{dC_m}{d\delta} S\bar{c} \frac{\rho V^2}{2}$

[redacted]

M_q $\quad C_{m_q} S\bar{c} \frac{\bar{c}}{2V} \frac{\rho V^2}{2}$

$M_{\dot{\alpha}}$ $\quad C_{m_{\dot{\alpha}}} S\bar{c} \frac{\bar{c}}{2V} \frac{\rho V^2}{2}$

Z_α $\quad -C_{L_\alpha} S \frac{\rho V^2}{2}$

Z_δ $\quad \frac{dC_L}{d\delta} S \frac{\rho V^2}{2}$

Subscript

t horizontal tail

TEST EQUIPMENT

The test airplane was a standard North American F-86A-5 with external booms added as shown in figures 1 and 2. The pertinent physical characteristics of the airplane are listed in table I.

Standard NACA optical instruments synchronized at 1/10-second intervals by a common timer were used to determine static and impact pressures on a Kollsman airspeed head mounted in the nose boom (fig. 2), normal acceleration at the center of gravity, pitching velocity, and elevator and stabilizer positions. The true Mach number and pressure altitude were obtained by correcting the static and impact pressures in accordance with the calibration of reference 1.

TEST PROCEDURE AND REDUCTION OF DATA

The flight program consisted entirely of elevator pulse-type maneuvers and covered a Mach number range of 0.60 to 1.04 with corresponding variations in trim lift coefficient of 0.35 to 0.12. The airplane was trimmed in either level or diving flight at the start of each run and, after application of the pulse, the control stick was returned approximately to the trim position and held against a chain stop so as to minimize any inadvertent elevator motion. The success of this system is shown in the typical flight records presented in figure 3. The pitching-velocity responses were analyzed by the method shown in appendix A.

All records at speeds greater than 0.92 Mach number were taken in diving flight. For the calculations presented herein, however, the altitude and Mach number were assumed to remain constant at their average values during the 2- to 4-second duration of each run. The validity of this assumption is borne out by the data shown in figure 3(a) wherein the Mach number does not vary over 0.7 percent during the interval in which the data were taken. The change in flight-path angle associated with a dive may have some effect on the response of the airplane; however, analytic investigation showed that in this case the effect on the period and damping of the oscillatory mode was negligible.

Since the actual flights covered an altitude range of 30,000 to 40,000 feet, the period and damping measurements were corrected to a standard altitude of 35,000 feet by assuming that the damping varies directly with the air density and that the period is inversely proportional to the square root of the density.

RESULTS AND DISCUSSION

The period of the oscillations as measured from flight records is plotted in figure 4 as a function of Mach number. It should be remembered that all the data presented herein were obtained in either level or diving flight, the lift coefficient varying between 0.35 and 0.12 at 35,000 feet over the speed range covered. It can be noted that there is a continuous decrease in period with increasing speed except for the slight rise between Mach numbers of 0.92 and 0.94. Also shown are values of period estimated from wind-tunnel data of reference 2 by the method shown in appendix B. The values computed from the wind-tunnel data are somewhat smaller in magnitude but show the same variation with speed as the test values of period.

Figure 5 shows a plot of damping coefficients that were obtained from the oscillation records by the method described in appendix A. Examination of this curve shows that, after reaching a peak value at a Mach number of 0.88, the damping drops sharply to a low value at 0.92, after which there is a sudden increase to a maximum at a Mach number of 0.94. Above 0.94 the damping decreases in an irregular fashion over the remainder of the test range. It should be noted that the sharp decrease in damping is defined by five separate test points taken independently at about Mach number 0.92. This is also the same speed at which the irregularity in the period was noted.

Also plotted in the same figure are estimated values of damping (see appendix B) which show somewhat smaller magnitudes over the range of Mach numbers covered by the wind tunnel. This difference may result from the assumptions made regarding both $d\epsilon/d\alpha$ (0.5) and the portion of M_q due to the wing and fuselage ($0.25\ M_{q_t}$).

Considerable scatter can be noted in the test points of figure 5. This is an indication of the difficulty involved in fairing an exponential envelope to the test data. The accuracy of the measurements is poorer at the lower speeds because the oscillations were almost completely damped within one cycle. It was very difficult to determine the damping from these test measurements at Mach numbers below 0.70. At the higher speeds (above Mach number 1.0) the scatter is not due entirely to inaccurate measurements since the records consisted of two or more well-defined cycles. The period measurements appear to be more consistent and no difficulty was encountered except at the lowest test speeds.

The period and damping test data (figs. 4 and 5) were used to compute the static stability parameter C_{m_α} shown in figure 6. The flight-test curve shows a rapid increase in static stability with increasing Mach number except for a dip, which is similar to that previously noted in figure 4.

The computed values of C_{m_α} should have the same degree of accuracy as the original period measurements since the period of oscillation depends almost entirely on C_{m_α}. As indicated in appendix A, however, a small error was introduced by the omission of the term $Z_\alpha M_q/mVI_y$; but in this case the error was estimated to be negligible at high speeds and less than 4 percent at the lowest test speed.

Also plotted in figure 6 are values of C_{m_α} obtained from the data of reference 2. There is fair agreement between the two curves, although the wind-tunnel results do show higher values of static stability corresponding to a shift in neutral point of about 2.5 percent.

The variation of $C_{m_q} + C_{m_{\dot{\alpha}}}$ with Mach number is plotted in figure 7. This parameter was computed by combining experimental values of damping coefficient b taken from the faired curve of figure 5 with values of C_{L_α} taken from figure 8.[1] These calculations are explained in appendix A.

By comparing figures 5 and 7, it can be seen that both curves exhibit the same general characteristics at Mach numbers greater than 0.92. At the lower speeds, however, the influence of C_{L_α} causes the total damping b to increase with Mach number, while the term $C_{m_q} + C_{m_{\dot{\alpha}}}$ is actually decreasing. The sudden drop in b at Mach number 0.88 is due also,

[1]Figure 8 is the result of estimations made by the North American Aviation Company based on wind-tunnel (reference 2) and transonic-bump tests.

[redacted]

at least partially, to the decrease in C_{L_α} that occurs at this same speed.

Also plotted in figure 7 is the variation of $C_{m_q} + C_{m_{\dot{\alpha}}}$ estimated from reference 2. Since the same values of C_{L_α} were used in computing both curves in this figure, the poor agreement between the two is the result of discrepancies between the estimated and the experimental damping coefficients shown in figure 5. In general, the accuracy to which $C_{m_q} + C_{m_{\dot{\alpha}}}$ can be determined experimentally is limited by the accuracies of both b and C_{L_α}. As shown in appendix A, $C_{m_q} + C_{m_{\dot{\alpha}}}$ is proportional to the difference between b and Z_α/mV and thus will usually be less accurate than either of these two quantities. Examination of the wind-tunnel data used in this report shows that Z_α/mV is approximately one-half as large as b; thus a 1-percent error in b results in a 2-percent error in $C_{m_q} + C_{m_{\dot{\alpha}}}$.

In figure 9 is plotted the number of cycles required for the oscillations to damp to 1/10 amplitude. The curve shows that below a Mach number of 0.85, approximately 0.95 cycle is required. Above this speed the number of cycles required increases rapidly with Mach number, exhibiting irregularities similar to those noted in the damping curve.

Ames Aeronautical Laboratory,
National Advisory Committee for Aeronautics,
Moffett Field, Calif.

[redacted]

APPENDIX A

METHOD OF ANALYSIS

For the analysis used in this report, the following longitudinal equations of motion are assumed:

$$mV\,(\dot{\alpha} - q) = Z_{\alpha}\alpha + Z_{\delta}\delta \tag{A1}$$

$$I_y\,\dot{q} = M_{\alpha}\alpha + M_{\dot{\alpha}}\dot{\alpha} + M_q q + M_{\delta}\delta \tag{A2}$$

Solving the two equations simultaneously for q/δ yields

$$\frac{q}{\delta} = \frac{C_1 D + C_o}{D^2 + bD + k} \tag{A3}$$

where

$$D = \frac{d}{dt} \tag{A4}$$

$$C_o = \frac{Z_{\delta}M_{\alpha} - M_{\delta}Z_{\alpha}}{mV\,I_y} \tag{A5}$$

$$C_1 = \frac{Z_{\delta}M_{\dot{\alpha}}}{mVI_y} + \frac{M_{\delta}}{I_y} \tag{A6}$$

$$b = -\frac{Z_{\alpha}}{mV} - \frac{M_q}{I_y} - \frac{M_{\dot{\alpha}}}{I_y} = \text{damping coefficient} \tag{A7}$$

$$k = \frac{Z_{\alpha}M_q}{mVI_y} - \frac{M_{\alpha}}{I_y} = \text{aerodynamic restoring moment} \tag{A8}$$

[redacted]

The damping coefficient b can be obtained from a typical oscillation record such as shown in figure 10 where the equation of the envelope is assumed to be of the form

$$a = e^{-\frac{b}{2}t} \tag{A9}$$

Thus

$$\frac{b}{2} = \frac{\ln(a_1/a_2)}{t_2 - t_1} \tag{A10}$$

The aerodynamic restoring moment k is determined from the period of the oscillation as follows:

$$P = \frac{2\pi}{\sqrt{k - \left(\frac{b}{2}\right)^2}} \tag{A11}$$

and, by rearranging terms,

$$k = \left(\frac{2\pi}{P}\right)^2 + \left(\frac{b}{2}\right)^2 \tag{A12}$$

The term C_{m_α} can be determined from k by using equation (A8), omitting the term $Z_\alpha M_q/mVI_y$. Investigation has shown that, in this case, this term is very small compared to M_α/I_y. Thus,

$$k = -\frac{M_\alpha}{I_y} = -C_{m_\alpha}\frac{Sc}{I_y}\frac{\rho V^2}{2} \tag{A13}$$

and

$$C_{m_\alpha} = -\frac{kI_y}{Sc}\frac{2}{\rho V^2} \tag{A14}$$

The damping factor $C_{m_q} + C_{m_{\dot{\alpha}}}$ can be obtained from equation (A7) using known values of b and C_{L_α}.

[redacted]

$$\frac{1}{I_y}\left(M_q + M_{\dot{\alpha}}\right) = -\frac{Z_\alpha}{mV} - b \tag{A15}$$

$$C_{m_q} + C_{m_{\dot{\alpha}}} = \frac{4I_y}{\rho VSc^2}\left(C_{L_\alpha}\frac{\rho VS}{2m} - b\right) \tag{A16}$$

The term $C_{1/10}$ is obtained from the relation

$$C_{1/10} = \frac{\ln 10}{P\frac{b}{2}} \tag{A17}$$

APPENDIX B

ESTIMATION OF DYNAMIC STABILITY PARAMETERS FROM STATIC WIND-TUNNEL TESTS

In general, it is not possible to obtain dynamic stability parameters directly from static wind-tunnel tests. By making certain assumptions, however, it was possible to estimate the values of the coefficients b and k using the data of reference 2; then the other stability parameters were computed by the methods of appendix A.

In appendix A it was shown that

$$b = -\frac{Z_\alpha}{mV} - \frac{M_q}{I_y} - \frac{M_{\dot{\alpha}}}{I_y}$$

$$k = \frac{Z_\alpha M_q}{mVI_y} - \frac{M_\alpha}{I_y}$$

To determine b and k it was necessary to evaluate Z_α, M_q, $M_{\dot{\alpha}}$, and M_α using wind-tunnel plots of C_{L_α}, dC_m/di_t, and dC_m/dC_L. This was done as follows:

For Z_α,

$$Z_\alpha = -C_{L_\alpha}\frac{\rho V^2}{2}S$$

For M_q, the portion of M_q due to the tail alone can be expressed as

$$M_{q_t} = -\eta_t \frac{dC_{L_t}}{d\alpha_t}\frac{\rho V S_t l_t^2}{2}$$

and since

$$\frac{dC_m}{di_t} = -\eta_t \frac{dC_{L_t}}{d\alpha_t}\frac{l_t S_t}{S\bar{c}}$$

then

$$M_{q_t} = \frac{dC_m}{di_t} \frac{\rho V S \bar{c} l_t}{2}$$

In addition, however, the portion of M_q due to the wing and fuselage must also be estimated; in this case, it was assumed to be 25-percent of M_{q_t}. Therefore,

$$M_q = 1.25 \frac{dC_m}{di_t} \frac{\rho V S \bar{c} l_t}{2}$$

For $M_{\dot{\alpha}}$, $M_{\dot{\alpha}}$ can be expressed as

$$M_{\dot{\alpha}} = -\eta_t \frac{dC_{L_t}}{d\alpha_t} \frac{d\epsilon}{d\alpha} \frac{\rho V S_t l_t^2}{2}$$

or

$$M_{\dot{\alpha}} = M_{q_t} \frac{d\epsilon}{d\alpha}$$

The term $d\epsilon/d\alpha$ was estimated to be 0.5 over the wind-tunnel speed range.

For M_α, M_α can be obtained from the plot of dC_m/dC_L in reference 2 where C_m is the moment coefficient about the quarter-chord point. The center of gravity of the test airplane was located at approximately 22.5 percent of the mean aerodynamic chord. Thus,

$$C_{m_\alpha} = C_{L_\alpha} \left(\frac{dC_m}{dC_L} - 0.025 \right)$$

and

$$M_\alpha = C_{m_\alpha} \frac{\rho}{2} V^2 S \bar{c}$$

[redacted]

REFERENCES

1. Thompson, Jim Rogers, Bray, Richard S., and Cooper, George E.: Flight Calibration of Four Airspeed Systems on a Swept-Wing Airplane at Mach Numbers Up to 1.04 by the NACA Radar-Phototheodolite Method. NACA RM A50H24, 1950.

2. Morrill, Charles P., Jr., and Boddy, Lee E.: High-Speed Stability and Control Characteristics of a Fighter Airplane Model With a Swept-Back Wing and Tail. NACA RM A7K28, 1948.

[redacted]

TABLE I.- PHYSICAL CHARACTERISTICS OF TEST AIRPLANE

Wing	
Total area (including flaps, slats, and 49.92 sq ft covered by fuselage	287.9 sq ft
Span	37.1 ft
Aspect ratio	4.79
Taper ratio	0.51
Mean aerodynamic chord (wing station 98.7 in. measured normal to center line)	97.03 in.
Sweepback of 0.25-chord line	35°14'
Root airfoil section (normal to 0.25-chord line)	NACA 0012-64 (modified)
Tip airfoil section (normal to 0.25-chord line)	NACA 0011-64 (modified)
Horizontal Tail	
Total area (including 1.20 sq ft covered by fuselage	35.0 sq ft
Span	12.8 ft
Aspect ratio	4.65
Taper ratio	0.45
Mean aerodynamic chord (horizontal-tail station 33.54 in.)	34.7 in.
Sweepback of 0.25-chord line	34°35'
Airfoil section (parallel to center line)	NACA 0010-64
Tail length	18.12 ft
Weight and corresponding center-of-gravity position (landing gear retracted)	
Take-off (c.g. at 23.0-percent M.A.C.)	14,102 lb
Landing (c.g. at 21.9-percent M.A.C.)	11,612 lb
Average for computation purposes (c.g. at 22.5-percent M.A.C.	12,800 lb
Average moment of inertia about Y axis	17,480 slug-ft^2

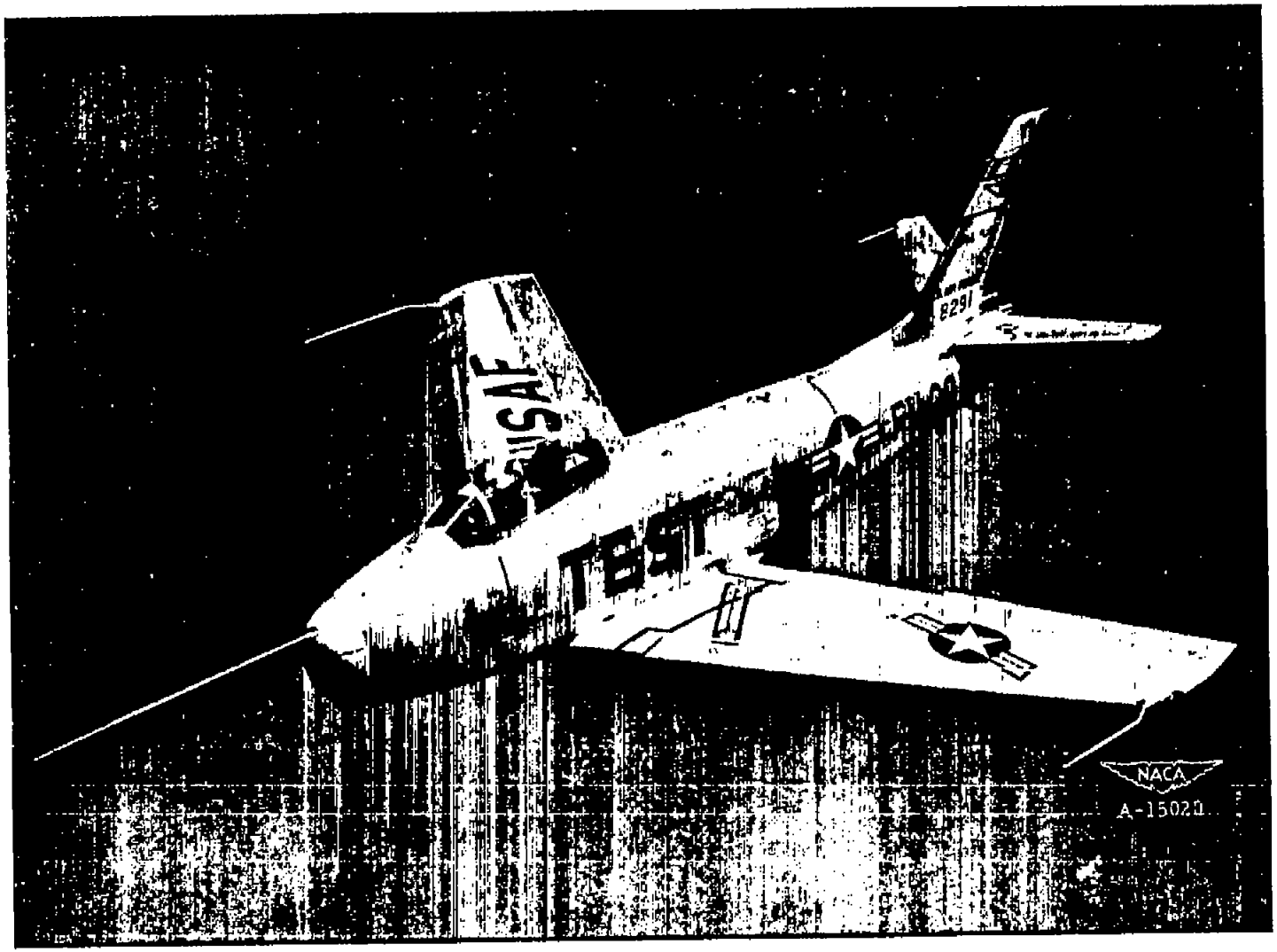

Figure 1.– Photograph of test airplane showing external boom configuration.

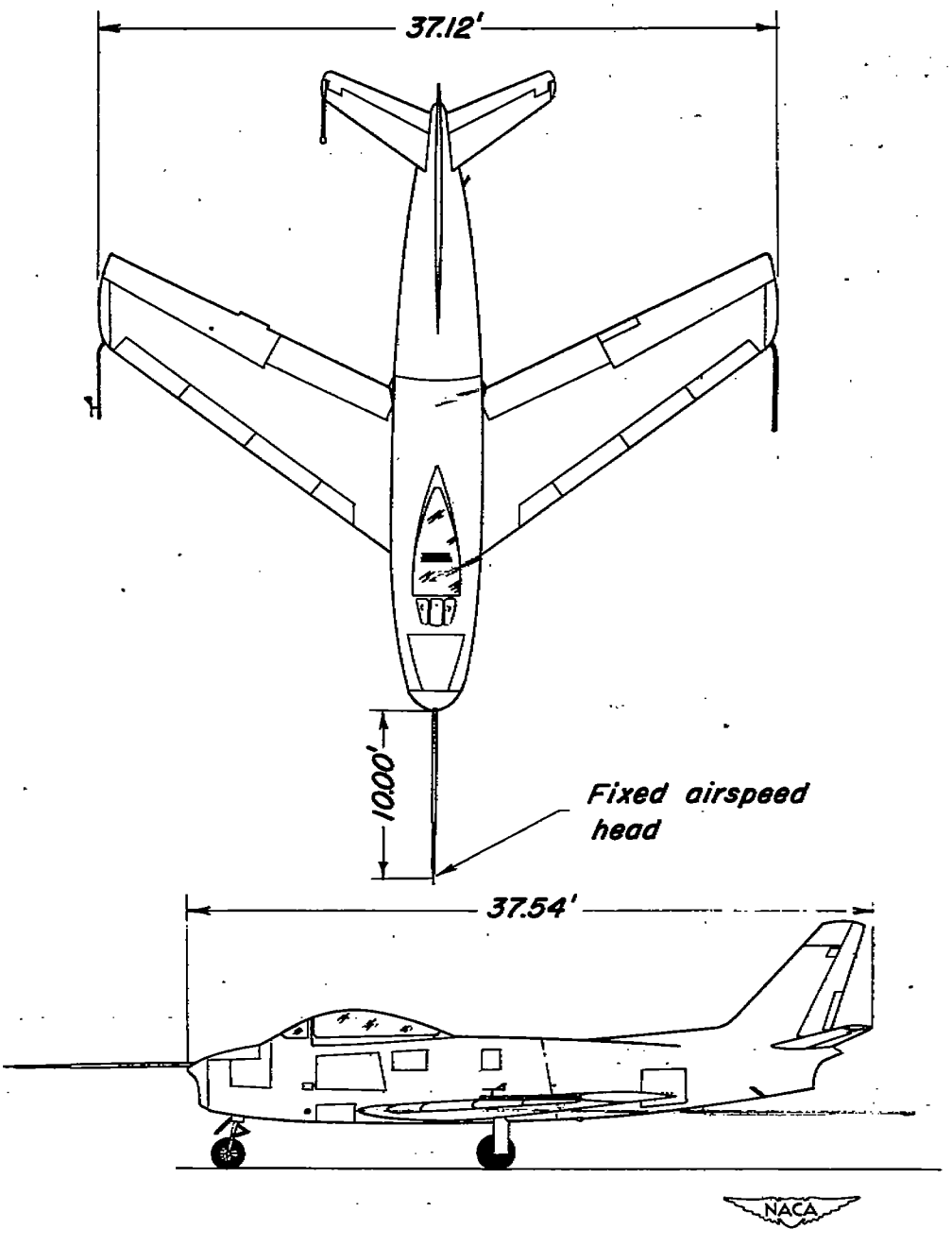

Figure 2.-Two-view drawing of test airplane showing research airspeed installation.

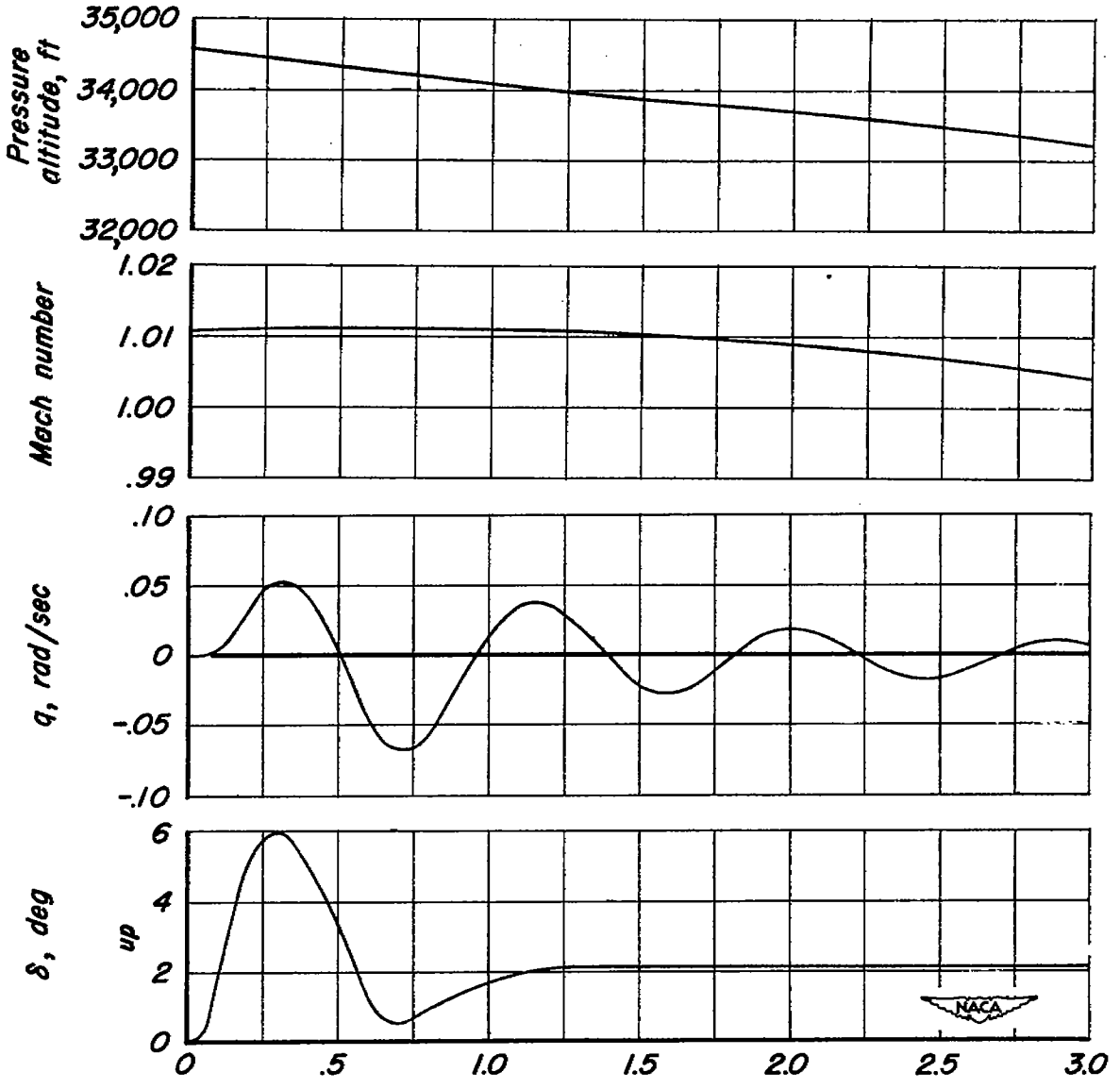

(a) M = 1.01 .

Figure 3.– Sample flight records of pressure altitude, Mach number, pitching velocity, and elevator angle.

[redacted]

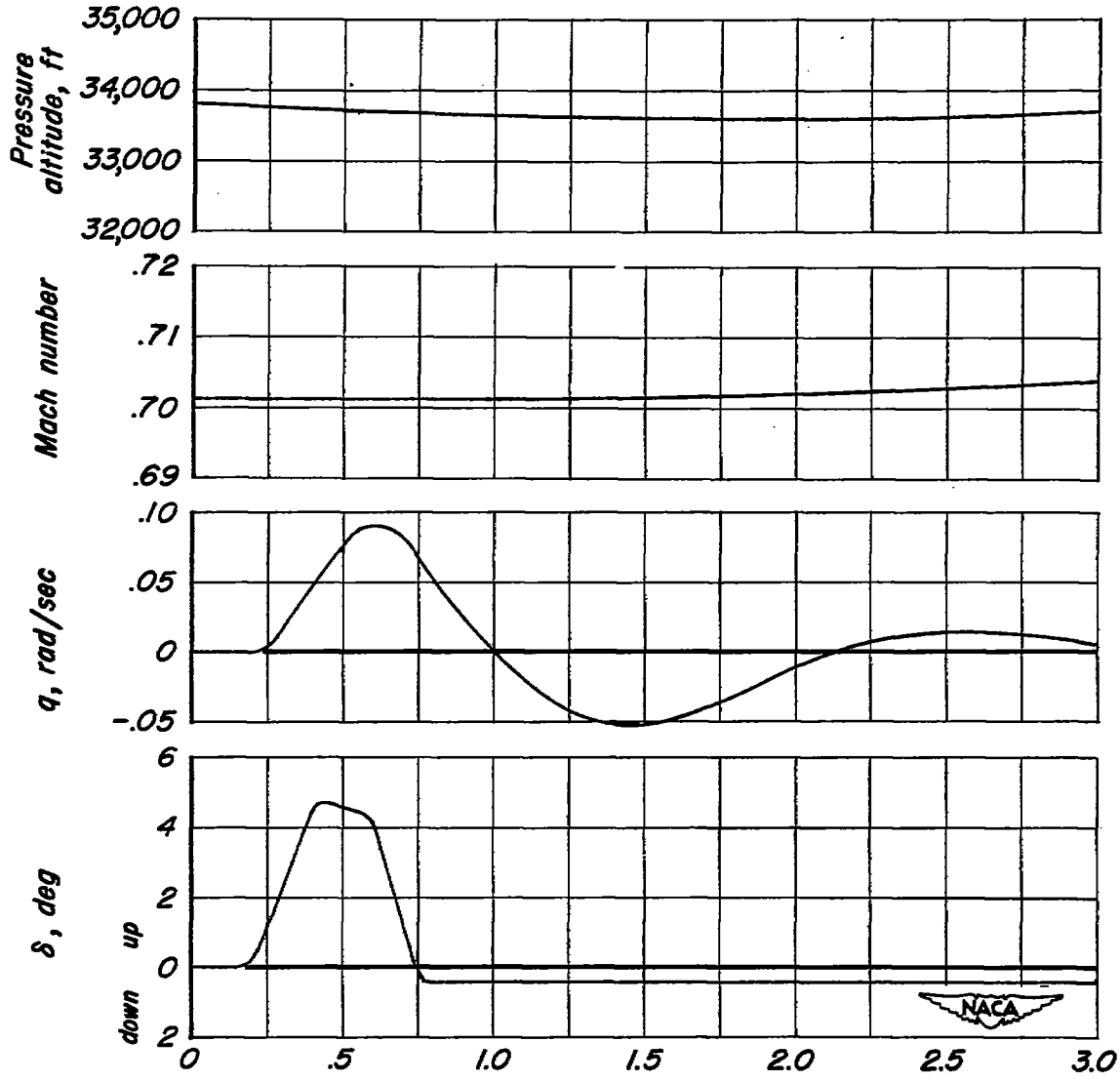

(b) M = 0.70 .

Figure 3.- Concluded.

[redacted]

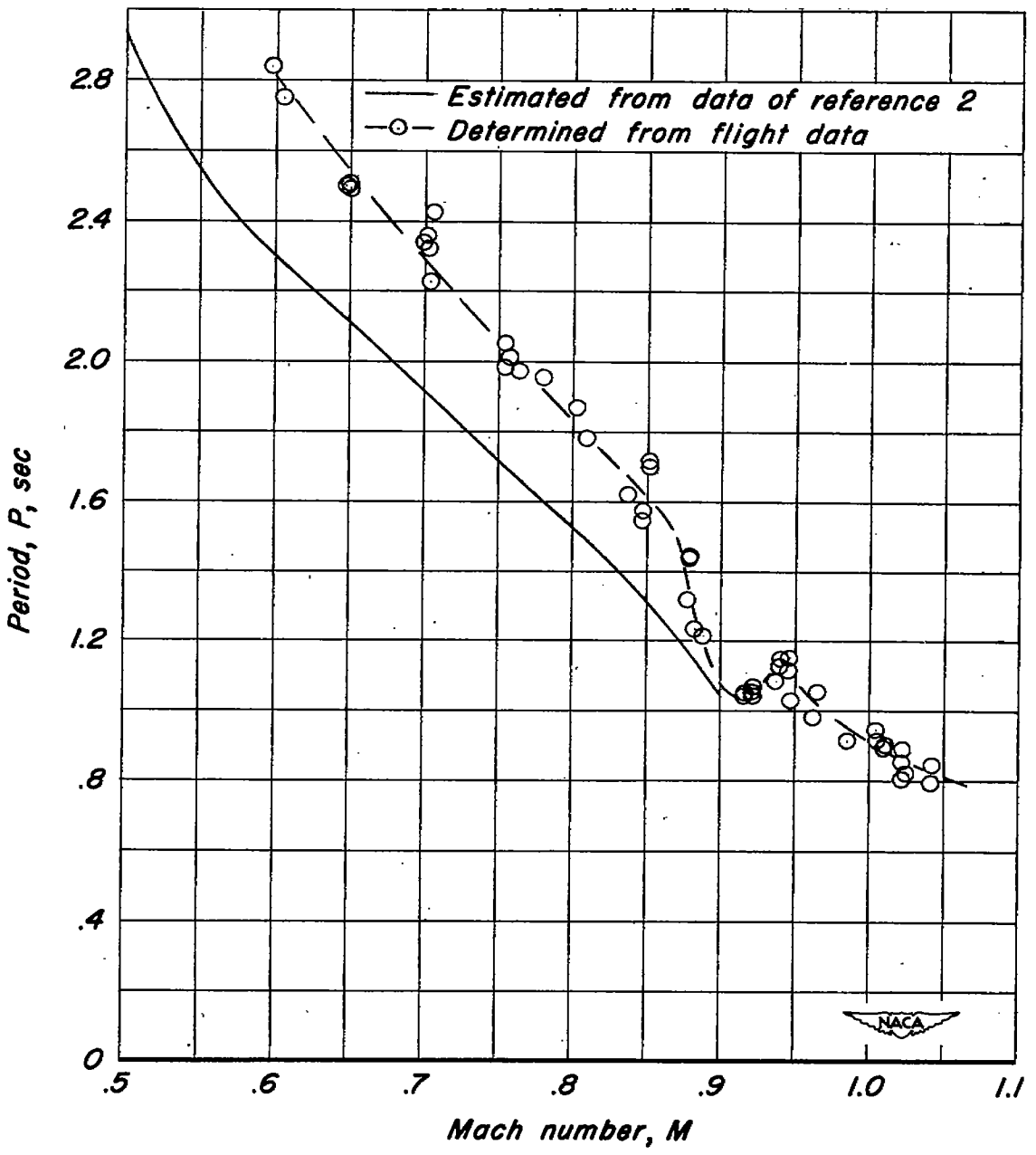

Figure 4.- Variation of period of oscillation with Mach number.

[redacted]

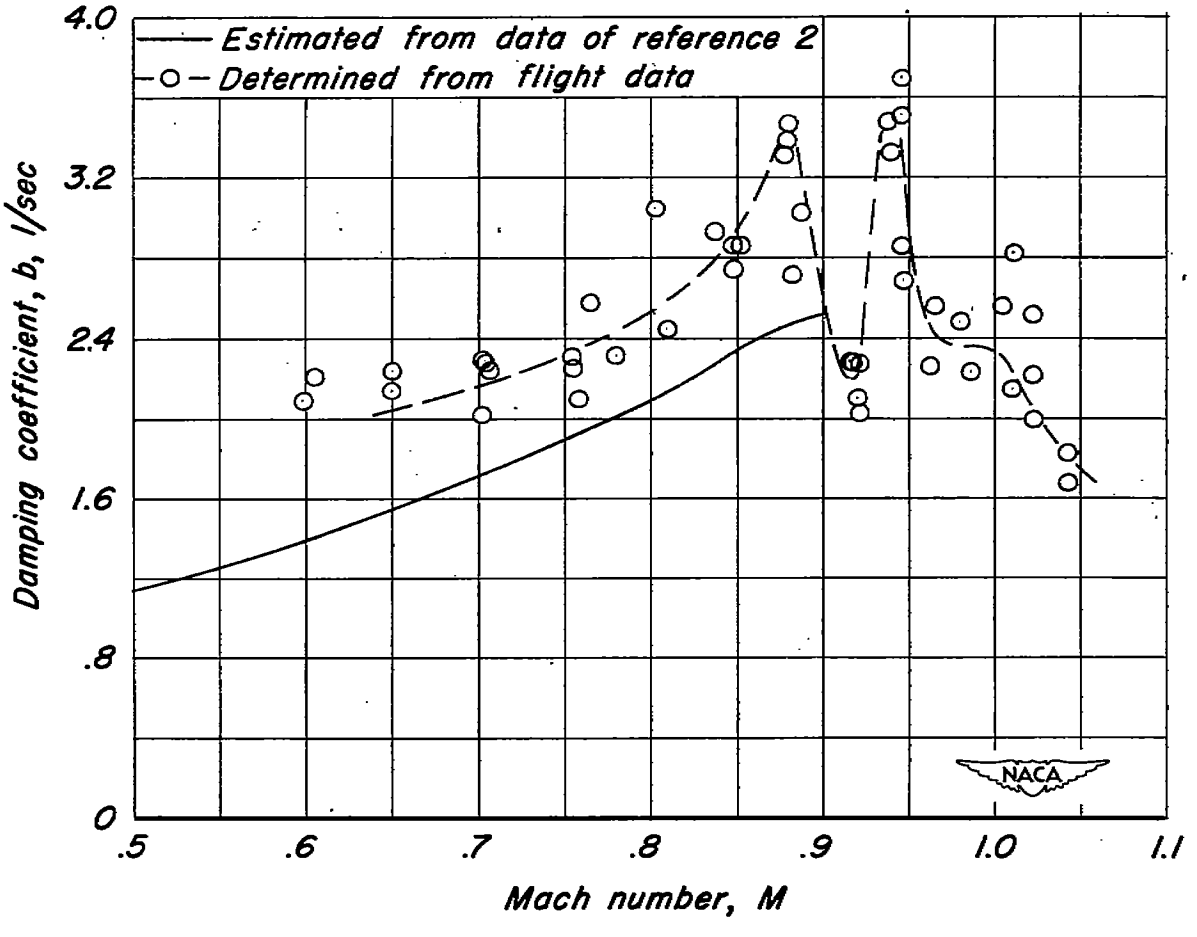

Figure 5.- Variation of damping coefficient with Mach number.

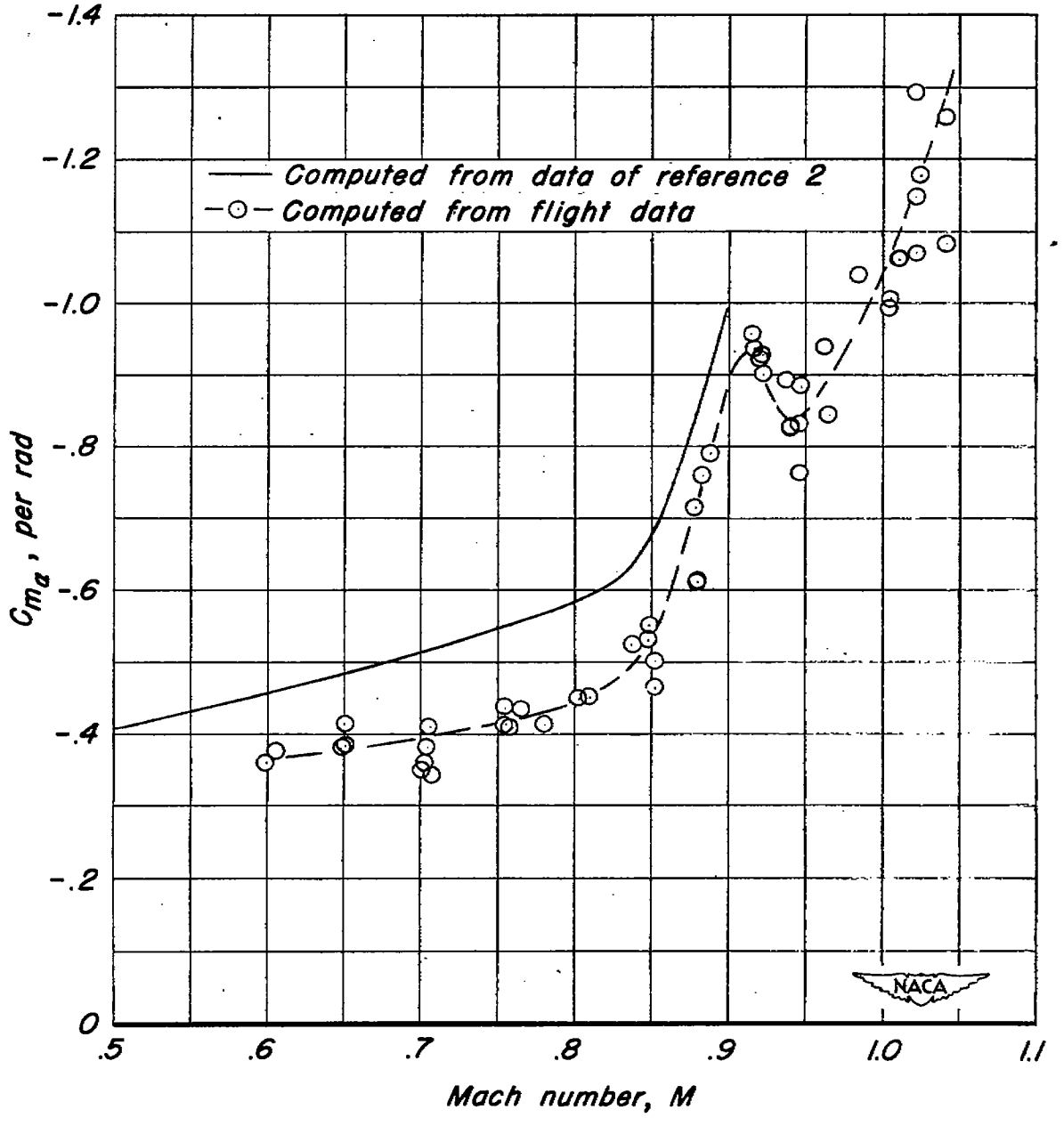

Figure 6.- Variation of C_{m_α} with Mach number.

[redacted]

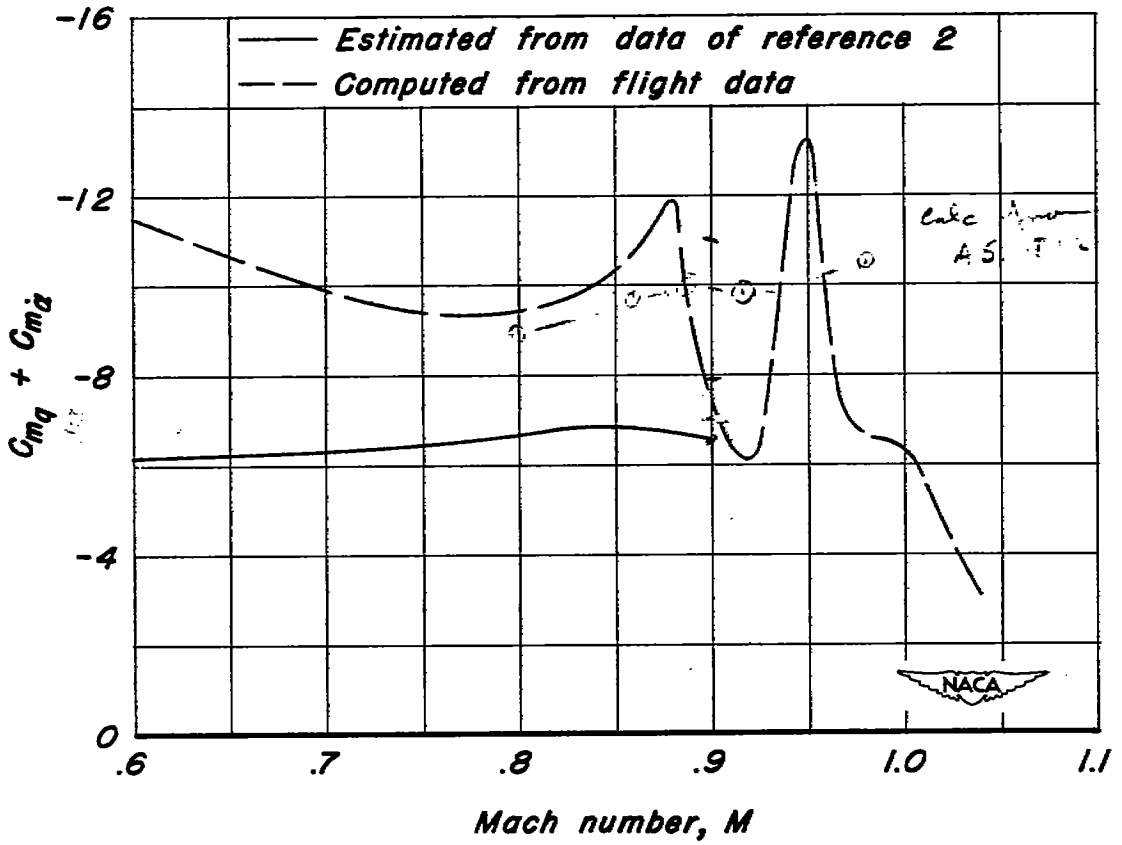

Figure 7.- Variation of $C_{m_q} + C_{m_{\dot{\alpha}}}$ with Mach number.

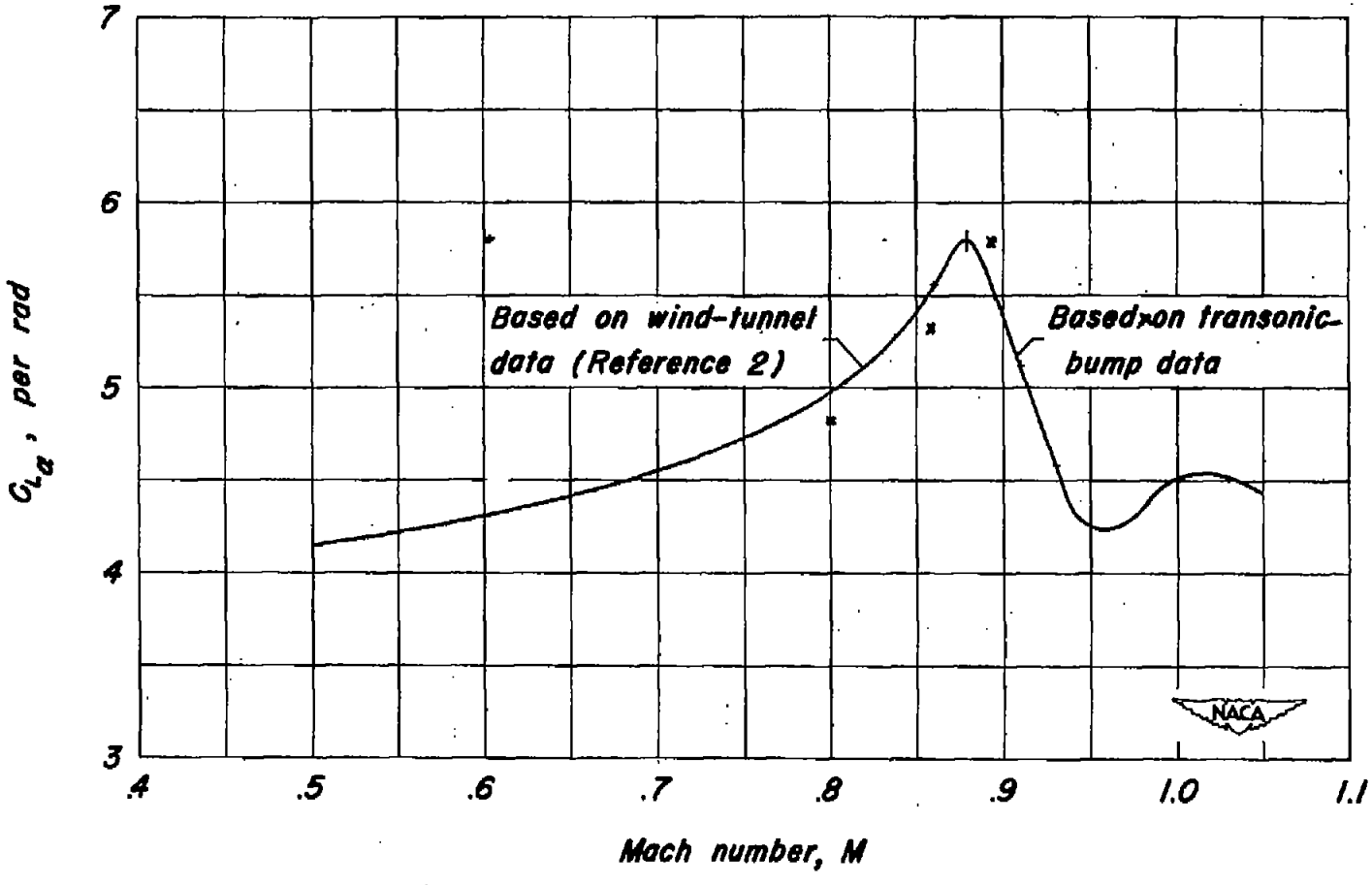

Figure 8.- Manufacturer's estimates of the variation with Mach number of lift-curve slope for steady flight lift coefficients.

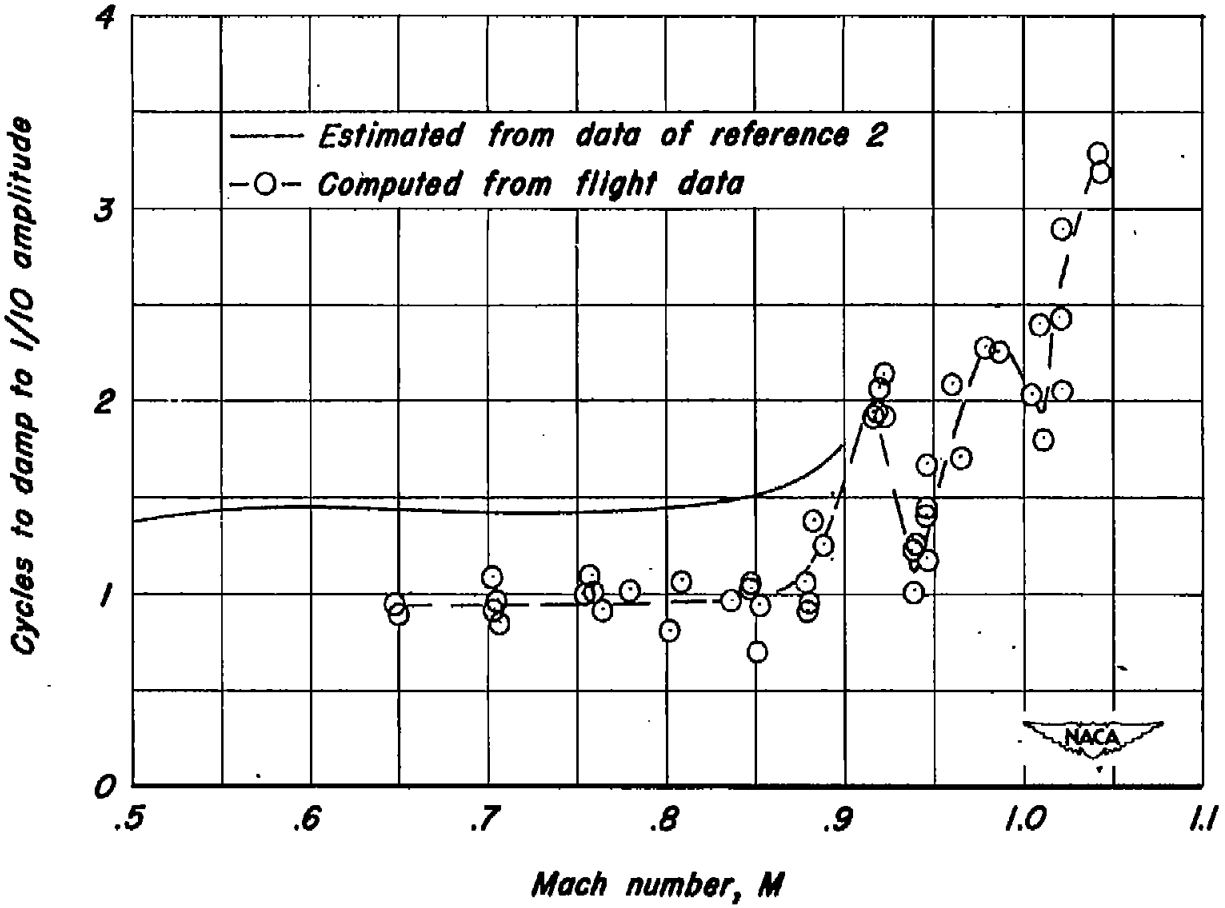

Figure 9.- Number of cycles required for oscillation to damp to 1/10 amplitude.

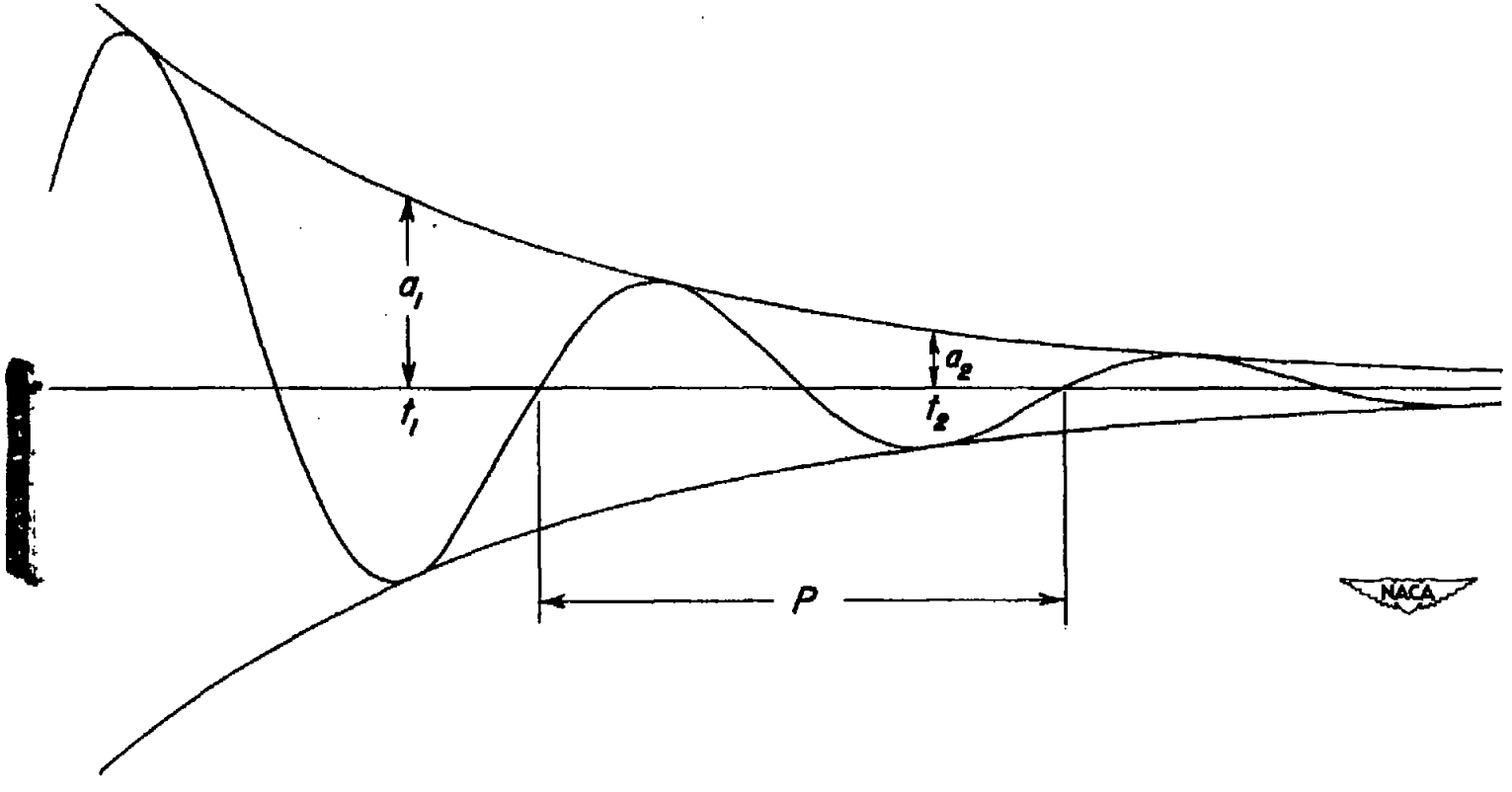

Figure 10.– Definition of terms used in the analysis of a typical oscillation.

NACA-Langley - 12-11-50 - 300